Self-optimized metal coatings for fiber plasmonics by electroless deposition

A. Bialiayeu,[1,*] C. Caucheteur,[3] N. Ahamad,[2] A. Ianoul,[2] and J. Albert[1]

[1]*Department of Electronics, Carleton University, 1125 Colonel By Drive, K1S 5B6 Ottawa, Canada*
[2]*Department of Chemistry, Carleton University, 1125 Colonel By Drive, K1S 5B6 Ottawa, Canada*
[3]*Université de Mons, Electromagnetism and Telecom Unit, Place du Parc 20, 7000 Mons, Belgium*
**alexbeliaev@gmail.com*

Abstract: We present a novel method to prepare optimized metal coatings for infrared Surface Plasmon Resonance (SPR) sensors by electroless plating. We show that Tilted Fiber Bragg grating sensors can be used to monitor in real-time the growth of gold nano-films up to 70 nm in thickness and to stop the deposition of the gold at a thickness that maximizes the SPR (near 55 nm for sensors operating in the near infrared at wavelengths around 1550 nm). The deposited films are highly uniform around the fiber circumference and in spite of some nanoscale roughness (RMS surface roughness of 5.17 nm) the underlying gratings show high quality SPR responses in water.

OCIS codes: (060.2370) Fiber optics sensors; (240.6680) Surface plasmons.

References and links

1. B. Lee, S. Roh, and J. Park, "Current status of micro- and nano-structured optical fiber sensors," Opt. Fiber Technol. **15**(3), 209–221 (2009).
2. K. S. Lee and T. Erdogan, "Fiber mode coupling in transmissive and reflective tilted fiber gratings," Appl. Opt. **39**(9), 1394–1404 (2000).
3. G. Laffont and P. Ferdinand, "Tilted short-period fibre-Bragg-grating-induced coupling to cladding modes for accurate refractometer," Meas. Sci. Technol. **12**(7), 765–770 (2001).
4. C. F. Chan, C. Chen, A. Jafari, A. Laronche, D. J. Thomson, and J. Albert, "Optical fiber refractometer using narrowband cladding-mode resonance shifts," Appl. Opt. **46**(7), 1142–1149 (2007).
5. Y. Shevchenko, C. Chen, M. A. Dakka, and J. Albert, "Polarization-selective grating excitation of plasmons in cylindrical optical fibers," Opt. Lett. **35**(5), 637–639 (2010).
6. Y. Y. Shevchenko and J. Albert, "Plasmon resonances in gold-coated tilted fiber Bragg gratings," Opt. Lett. **32**(3), 211–213 (2007).
7. J. Homola, "Surface plasmon resonance sensors for detection of chemical and biological species," Chem. Rev. **108**(2), 462–493 (2008).
8. T. Guo, H. Y. Tam, P. A. Krug, and J. Albert, "Reflective tilted fiber Bragg grating refractometer based on strong cladding to core recoupling," Opt. Express **17**(7), 5736–5742 (2009).
9. K. Matsubara, S. Kawata, and S. Minami, "Optical chemical sensor based on surface plasmon measurement," Appl. Opt. **27**(6), 1160–1163 (1988).
10. R. Jorgenson and S. Yee, "A fiber-optic chemical sensor based on surface plasmon resonance," Sens. Actuators B Chem. **12**(3), 213–220 (1993).
11. J. Pollet, F. Delport, K. P. Janssen, K. Jans, G. Maes, H. Pfeiffer, M. Wevers, and J. Lammertyn, "Fiber optic SPR biosensing of DNA hybridization and DNA-protein interactions," Biosens. Bioelectron. **25**(4), 864–869 (2009).
12. H. Raether, "Surface plasma oscillations as a tool for surface examinations," Surf. Sci. **8**(1-2), 233–246 (1967).
13. P. Adam, J. Dostalek, and J. Homola, "Multiple surface plasmon spectroscopy for study of biomolecular systems," Sens. Actuators B Chem. **113**(2), 774–781 (2006).
14. G. Meltz, S. J. Hewlett, and J. D. Love, "Fiber grating evanescent-wave sensors," Proc. SPIE **2836**, 342–350 (1996).
15. R. Slavík, J. Homola, J. Čtyroký, and E. Brynda, "Novel spectral fiber optic sensor based on surface plasmon resonance," Sens. Actuators B Chem. **74**(1-3), 106–111 (2001).
16. T. Allsop, R. Neal, S. Rehman, D. J. Webb, D. Mapps, and I. Bennion, "Characterization of infrared surface plasmon resonances generated from a fiber-optical sensor utilizing tilted Bragg gratings," J. Opt. Soc. Am. B **25**(4), 481–490 (2008).

#151467 - $15.00 USD Received 20 Jul 2011; revised 27 Aug 2011; accepted 27 Aug 2011; published 12 Sep 2011

17. G. Nemova and R. Kashyap, "Fiber-Bragg-grating-assisted surface plasmon-polariton sensor," Opt. Lett. **31**(14), 2118–2120 (2006).
18. Y.-J. He, Y.-L. Lo, and J.-F. Huang, "Optical-fiber surface-plasmon-resonance sensor employing long-period fiber gratings in multiplexing," J. Opt. Soc. Am. B **23**(5), 801–811 (2006).
19. S. Mani Tripathi, E. Marin, A. Kumar, and J.-P. Meunier, "Refractive index sensing characteristics of dual resonance long period gratings in bare and metal-coated D-shaped fibers," Appl. Opt. **48**(31), 53–58 (2009).
20. B. Špačková and J. Homola, "Theoretical analysis of a fiber optic surface plasmon resonance sensor utilizing a Bragg grating," Opt. Express **17**(25), 23254–23264 (2009).
21. C. Caucheteur, Y. Shevchenko, L. Y. Shao, M. Wuilpart, and J. Albert, "High resolution interrogation of tilted fiber grating SPR sensors from polarization properties measurement," Opt. Express **19**(2), 1656–1664 (2011).
22. V. Voisin, C. Caucheteur, P. Mégret, and J. Albert, "Interrogation technique for TFBG-SPR refractometers based on differential orthogonal light states," Appl. Opt. **50**(22), 4257–4261 (2011).
23. S. Roh, H. Kim, and B. Lee, "Infrared surface plasmon resonance in a subwavelength metallic grating under illumination at a large incidence angle," J. Opt. Soc. Am. B **28**(7), 1661–1667 (2011).
24. W.-J. Lee, J.-E. Kim, H. Y. Park, S. Park, M.-S. Kim, J. T. Kim, and J. J. Ju, "Optical constants of evaporated gold films measured by surface plasmon resonance at telecommunication wavelengths," J. Appl. Phys. **103**(7), 073713 (2008).
25. Y. Lo, Y. Lin, and Y. Chen, "Athermal fibre Bragg grating strain gauge with metal coating in measurement of thermal expansion coefficient," Sens. Actuators A Phys. **117**(1), 103–109 (2005).
26. Y. Feng, H. Zhang, Y.-L. Li, and C.-F. Rao, "Temperature sensing of metal-coated fiber bragg grating," IEEE/ASME Trans. Mechatron. **15**(4), 511–519 (2010).
27. S. Hrapovic, Y. Liu, G. Enright, F. Bensebaa, and J. H. T. Luong, "New strategy for preparing thin gold films on modified glass surfaces by electroless deposition," Langmuir **19**(9), 3958–3965 (2003).
28. J. Kimling, M. Maier, B. Okenve, V. Kotaidis, H. Ballot, and A. Plech, "Turkevich method for gold nanoparticle synthesis revisited," J. Phys. Chem. B **110**(32), 15700–15707 (2006).
29. M. Perez, "Gibbs–Thomson effects in phase transformations," Scr. Mater. **52**(8), 709–712 (2005).
30. E. Fontana, "Thickness optimization of metal films for the development of surface-plasmon-based sensors for nonabsorbing media," Appl. Opt. **45**(29), 7632–7642 (2006).

1. Introduction

Chemical sensing using optical fibers is a growing field of research because of the fiber inertness, compact size and the multiple modalities offered by variations in the power and spectrum of the light sources used (see reference [1] for instance). One of these modes of operation is surface Plasmon resonance (SPR), a phenomenon that can be observed on metal surfaces (including coated optical fibers). In order to optimize the SPR sensitivity and resolution, the metal coating thickness and uniformity must be controlled very accurately around the fiber circumference, for thicknesses of the order of a few tens of nm. For coatings that are too thin, the SPR resonances broaden and weaken. On the other hand, when the thickness is too large, light cannot tunnel across the metal to excite the Plasmon polariton on the outer surface. Fine deposition control is difficult to achieve on small diameter cylindrical fibers and we propose here a technique to monitor the metal film growth in situ as well as a quantitative tool to stop the coating process at the optimum thickness, even for unknown deposition rates. We use a Tilted Fiber Bragg Grating (TFBG) inscribed in the core of a single mode fiber to detect the growth of the metal coating during a wet chemical plating process. While the resulting coated TFBG can be used as a SPR sensor once the plating is completed, other types of fiber SPR sensors can be fabricated simultaneously in the same process reactor, as long as the sensor operating wavelengths are similar. The TFBG is then only used as a process monitor.

TFBGs belong to the short-period gratings family, with grating planes slightly tilted relative to the fiber cross-section. Such tilted gratings enhance light coupling from the fiber core to the backward-going cladding modes [2,3]. The coupling produces discrete narrow attenuation bands in the transmitted spectrum (the "resonances") and since the cladding modes are guided by the fiber-surrounding medium interface, these resonances are extremely sensitive to the refractive index of the surrounding medium [4]. Thus TFBGs can be used in chemical and biological applications [5–7]. It is possible to exploit the large differential sensitivity of the core and cladding modes to various perturbations to develop very accurate

#151467 - $15.00 USD Received 20 Jul 2011; revised 27 Aug 2011; accepted 27 Aug 2011; published 12 Sep 2011

fiber sensors with a unique set of advantages, including the possibility to isolate temperature effects and develop compact and robust refractometers with a wide operating range [4,8].

The TFBG sensor performance can be further improved by introduction of a nano-scale metal coating on its surface, thus allowing the further possibility of coupling to surface plasmon resonances (SPR) that can be used for chemical sensing [9].

Back in 1993, Jorgenson and Yee were the first to demonstrate fiber-based SPR sensors with a multimode fiber that had its cladding replaced with a metal coating [10]. The spectral attenuation of such fibers shows a distinct loss peak at wavelengths where the dominant propagating modes are phase matched to the SPR of the metal film (and thus lose power to the metal). This method is still in use today [11] but the use of multimode fiber requires accurate control of the modal repartition of the input launched power and the linewidths of the resonances are in the tens of nm at least. One approach to narrow SPR resonances is to use gratings in the structure to control the phase matching conditions between the input light and the surface polaritons [12,13] and this is also true for fiber-based SPR. In fibers, the use of a single mode core further removes the difficulty arising from multimodal dispersion and the use of gratings allow very accurate coupling to select cladding modes at unique wavelengths (as determined by phase matching conditions).

The first attempt to implement a single mode fiber grating chemical sensor was reported in 1996 by Meltz [14]. The idea was to polish away the fiber cladding to expose the evanescent field of the core to the medium outside. This was further explored in later years [15], including a combination of the exposed core with a TFBG and metal coating for SPR applications [16].

Grating-based, single-mode fiber SPR devices that do not require cladding shape modifications or removal were further proposed theoretically by Nemova and Kashyap for custom designed fiber geometries [17], and also theoretically by He *et al.* using long period gratings in normal fibers [18], followed by Tripathi [19] and Homola [20]. Finally, our group proposed and experimentally demonstrated the use of tilted fiber Bragg gratings in conventional, un-modified standard single mode fibers to excite SPR at infrared wavelengths [6]. More recent publications have confirmed many attractive features of the TFBG-SPR configuration and further demonstrated reproducible and high sensitivity refractometry based on polarization-dependent measurements [5,21,22].

The purpose of the present paper is to demonstrate that electroless plating of gold from solution is a simple and efficient way to deposit a conformal coating of the required thickness and uniformity for fiber SPR applications and furthermore that an in-fiber FBG can be used to monitor the deposition so that the plating can be stopped at the optimum film thickness for SPR. A quantitative measure of the quality of the SPR response of the TFBG in the plating solution is provided by tracking the polarization dependent loss in real time and used as a criterion to end the plating. Therefore, a precise control of the plating process (temperature, chemical concentrations) is not necessary and reproducible coatings with thicknesses of the order of 50 nm can be obtained regardless of the speed of the plating process.

2. Theoretical background

The cladding modes excited by TFBGs have nonzero evanescent field at the cladding boundary and they can tunnel outside of the fiber through the thin metal coating. When some modes (among the large number of cladding modes accessible) are phase matched to a SPR of the outer surface of the metal coating, the light energy incident from these cladding modes is efficiently coupled to the surface plasmon polariton [6]. The phase matching condition is relatively narrowband (5-10 nm) and involves only a small subset of cladding modes [6]. The energy coupled to the SPR causes a drastic change in the TFBG transmission spectrum at wavelengths corresponding to the resonant modes. The principle of operation of the TFBG SPR sensor is analogous to the well-known Kretschmann-Raether setup [9,12], except that the cladding modes use wavelength and angle scanning to probe for the SPR phase matching

#151467 - $15.00 USD Received 20 Jul 2011; revised 27 Aug 2011; accepted 27 Aug 2011; published 12 Sep 2011

condition (because each cladding mode couples at a different wavelength and "strikes" the cladding boundary at a different incident angle). Finally, a further increase of the selectivity of the modes coupling to SPR is provided by controlling the light polarization. It is well known that SPR excitation only occurs for TM polarized light [12], i.e. light polarized perpendicularly to the metal surface, but it is not so obvious how to generate radially polarized light inside an optical fiber. However, it was found recently that TFBGs couple to different families of cladding modes when the input core mode light is polarized along the tilt plane or at 90 degrees to it [5]. This discovery led the way to a strong increase in the accuracy with which we can follow SPR shifts associated with small refractive index changes of the outer medium surrounding the fiber by using the polarization dependent loss (PDL) of the TFBG transmission [21]. In particular, it was found that narrowband resonances (100 pm spectral bandwidth (BW)) with refractometric sensitivities (S) of 350 nm/RIU (refractive index units) showed up in the PDL spectrum. These resonances have some of the highest figures of merit (S/BW = 3500 RIU^{-1}) for SPR sensors of any kind [23].

Of course the key to all this is the ability to coat the fibers with a suitable metal film. The fact that we use a cylindrically symmetric fiber is quite advantageous in many aspects but makes the deposition of nanometer-scale thickness metal films that are uniform around the 125 μm diameter circumference of the fiber quite challenging. In the past we used a time calibrated two-step sputtering process [6,24] to deposit gold films on fibers but were facing some reproducibility issues that could only come from coating errors (the TFBG process itself is highly reproducible and uses well established industrial mass production methods). In an effort to improve this situation, we have investigated electroless plating [25], because of its potential for highly conformal metal coatings on non-planar surfaces, its low cost and simplicity of implementation (with a potential for batch production), and its relatively low deposition rate, which facilitates the control of the process duration.

It is the purpose of this paper to show that electroless gold coatings can be deposited reliably and accurately for the fabrication of near infrared TFBG-SPR sensors, but most importantly that the TFBG itself can be used to monitor the deposition process and to stop it at the optimum film thickness for SPR excitation of metal coated fibers in water. We further demonstrate that the electroless-deposited gold layer retains some significant granularity but that this granularity does not represent an impediment to the quality of the SPR resonances that we observe. While coating conventional FBGs with copper and nickel has been described earlier for the purpose of making the FBG response athermal, the exact thickness and the uniformity of the films was not critical for those applications [25]. Further studies of thermal stress between such metal coatings and optical fibers were performed in [26], where it was shown that the metal coating of FBG sensors can be used not only as a protective layer but also as a temperature sensitivity booster.

The method we use to coat the TFBG relies on the attachment of gold nanoparticles on a suitably prepared bare fiber surface, followed by a plating process that uses the nanoparticles to catalyze the deposition of further gold from solution, as described in [27]. During the deposition, we monitor the wavelengths and amplitudes of several resonances in the transmission spectrum to identify the appearance of the SPR signature. As a separate check, although this is not absolutely necessary for the fabrication of TFBG-SPR sensors, we further calibrated the monitoring process by performing Atomic Force Measurements (AFM) on sample films to correlate the TFBG response with the physical thickness of the films. The AFM measurements further provided evidence about the nanoscale granularity of the films and its potential impact on the quality of the surface Plasmon resonances.

2. Experiments

The 1-cm-long TFBGs with a tilt angle of 10° were inscribed in the hydrogen-loaded core of CORNING SMF-28 optical fiber using 248 nm pulsed KrF excimer laser and the phase mask technique. Typical conditions are: pulse energy density 100 mJ/cm^2 at the fiber, 100 Hz

#151467 - $15.00 USD Received 20 Jul 2011; revised 27 Aug 2011; accepted 27 Aug 2011; published 12 Sep 2011

repetition rate for two minutes, and grating period 554 nm. These conditions give grating strengths sufficient to couple 99% of the core light to cladding modes near 1550 nm as described in [4].

2.1.Procedure for electroless coating of the fiber

The metal film coating was performed using the electroless deposition method, based on the reduction of metallic ions from a solution to a solid surface without applying an electrical potential [27].

At the first step, the fiber surface was cleaned and prepared for chemical deposition. The plastic jacket around the fiber was removed by soaking it into dichloromethane (CH_2Cl_2) and further cleaned to remove organic residue through the following multistep approach. The uncoated area of the fiber was rinsed with methanol and subsequently treated with freshly prepared piranha solution (mixture of H_2O: NH_3: H_2O_2 = 5:1:1) at 70°C for 10 min followed by rinsing with de-ionized water.

The cleaned fiber was then submersed in a 1% (3-aminopropyl)trimethoxysilane (APTMS, Aldrich, 97%, 281778) in methanol for 20 minutes in order to form a uniform monolayer on the fiber surface. APTMS molecules assembled on the glass by covalently bonding to exposed hydroxyl sites (Si-OH) on the glass, thus forming a cross-linked self-assembled monolayer (SAM).

The APTMS modified fiber was rinsed with methanol and de-ionized water followed by drying with a flow of N_2 gas. After drying, the modified fiber was submerged into a freshly prepared colloidal solution of gold nanoparticles (synthesized by the method described by Turkevich [28]) for one hour. The colloidal gold nanoparticles attached on the amine head of APTMS by forming multiple chemical bonds.

Electroless deposition of gold was then performed as described in [27]. Briefly, the fiber modified with gold nanoparticles was dipped into the plating bath consisting of complex metal ions (freshly prepared 0.01% chloroauric acid, $HAuCl_4$) and a reducing agent (hydroxyl amine: NH_2OHCl, 0.4 mM). The fiber was left in the solution for 80 min without stirring. The Au nanoparticles immobilized on the glass surface constitute excellent sites for the reduction of Au (I) to Au (0) by the hydroxyl amine. Therefore, electroless plating occurs on the surface of already immobilized gold nanoparticles by forming closed packed enlarged nanoparticles that eventually merge into a somewhat continuous thin gold film.

For the purpose of an independent thickness correlation measurement, the plating process was monitored in control experiments where fiber samples were extracted at different time intervals, rinsed with de-ionized water, dried and then subjected to AFM analysis as follows.

The topography of the fiber surfaces were obtained using an Ntegra atomic force microscope in semi-contact mode in air at 23°C using 200 μm-long soft cantilevers with integrated pyramidal silicon nitride tips having a spring constant of 60 mN/m. The AFM images were further processed by the Nova image processing software and Matlab.

2.2. Optical setup

The process of gold film deposition was also continuously monitored in real-time by collecting the TFBG transmission spectra.

#151467 - $15.00 USD Received 20 Jul 2011; revised 27 Aug 2011; accepted 27 Aug 2011; published 12 Sep 2011

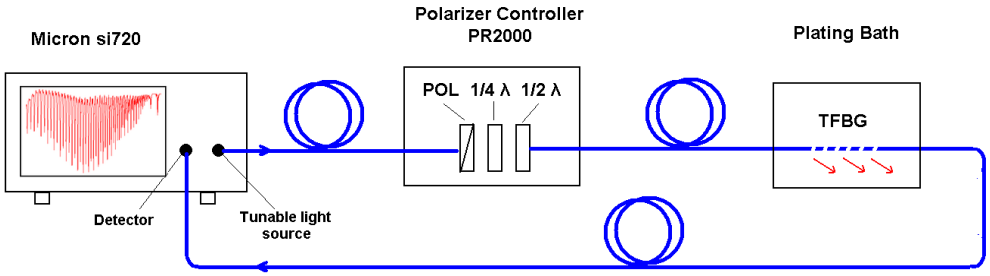

Fig. 1. Schematic of the optical experiment setup.

The experimental setup is shown schematically in Fig. 1. The transmission spectra of the TFBG sensor were acquired with the SI720 FBG interrogator from Micron Optics (made up of a fast sweeping tunable laser and integrated photodetector). A polarization controller (model PR2000 from JDS Uniphase) was inserted in the input light path between the source and the TFBG immersed in the plating bath. The polarization controller was set to continuously scan all linearly polarized light states in 80 seconds.

The spectra (over the full range from 1520 to 1570 nm) were taken continuously at a rate of one spectrum for each 0.2 seconds, which gave a polarization angle rotation of less than 1° during the acquisition of each full spectrum. Such high resolution allowed to collect a huge amount of data and as a result to precisely describe the TFBG-SPR sensor spectral and polarization response.

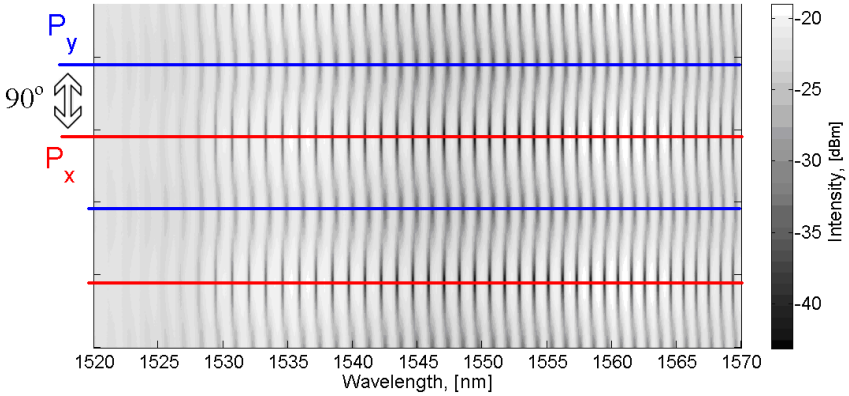

Fig. 2. Density plot representation of the TFBG spectra acquired as a function of time, near the beginning of the deposition, with continuously rotating polarization angle. The orthogonal polarizations states P_x and P_y are identified by the red and blue lines and the corresponding spectra can be extracted easily (either in quasi real-time or in post-processing).

3. Results and discussion

3.1 Process monitoring

The data collected during the experiments can be represented in the form of the density plot shown in Fig. 2, where each single spectrum becomes a horizontal line whose darkness corresponds to the attenuation in the TFBG sensor as a function of wavelength. These spectra were stacked together, forming a complete picture of the sensor response over the time of observation. It is clearly seen from the data subset shown in Fig. 2 that there are well defined periodically occurring extremes in the sensor response, corresponding to two states of linearly polarized light, separated from each other by 90 degrees of polarization angle (at this moment in time there is very little gold on the fiber). Since we are using non-polarization maintaining fiber, this polarization control can be achieved as long as the fiber is not severely twisted or

#151467 - $15.00 USD Received 20 Jul 2011; revised 27 Aug 2011; accepted 27 Aug 2011; published 12 Sep 2011

bent between the source, grating and detector (because then the input linear polarization remains linearly polarized, although at an arbitrary angle, when it reaches the grating). Since the polarization angle is continuously scanned, there is no need to pre-align the polarization states of the input light with the tilt plane of the grating or choosing particular origin of the polarization angle. All states of polarization are collected, and the orthogonal states are easily extracted from the data. The identification of the polarization states corresponding to the optimum orientations of the input light polarization relative to the tilt plane is done a posteriori, and can be constantly re-adjusted should the input conditions change (moving patch cords for instance). As shown in reference [5] one of these states couples to cladding modes that can excite plasmon resonances, while the other state couples to SPR-inactive modes.

It is now possible to simplify the sensor response analysis by extracting spectral data only for the two optimum linearly polarized orthogonal states P_x and P_y: a typical pair of spectra, extracted from the data of Fig. 2 is shown in Fig. 3.

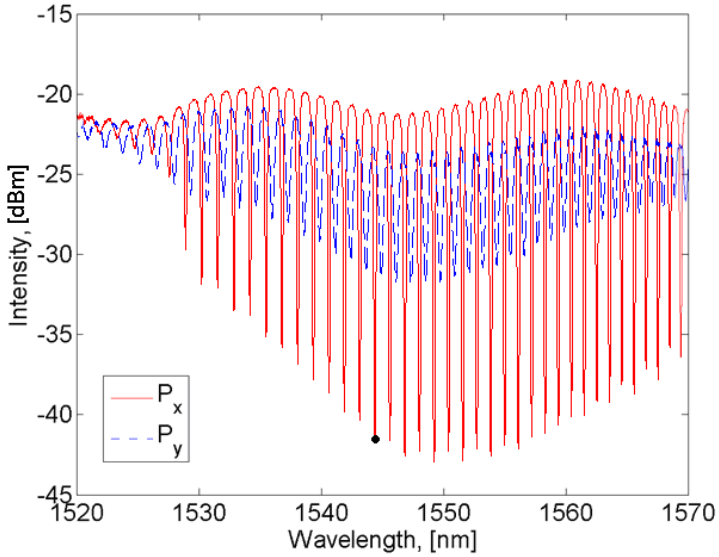

Fig. 3. TFBG spectra for orthogonal polarization states P_x and P_y, taken after 5 minutes of gold film deposition.

These spectra are quite complex and in order to further extract useful quantitative information, we proceed to show that the evolution of individual resonances can be correlated to the thickness growth. Figure 4 shows how the amplitude and wavelengths of a neighboring pair of individual resonances (identified by a dot on Fig. 3, and corresponding to orthogonal polarization states) evolve during plating. This evolution depends strongly on polarization, as can be expected from the deposition of a metal film at the cladding boundary: the effective indices and coupling coefficients of cladding modes depend on boundary conditions and modes with electric field mostly tangential at the cladding boundary will evolve differently from modes with mostly radial electric fields there. The strong variation in the sensor optical response can be easily detected and correlated with the growth of the metal film, provided that independent measurements of film thickness are carried out to calculate a calibration factor. The variations in the sensor response for the P_y polarization are the most rapid and thus most suitable for detection.

#151467 - $15.00 USD Received 20 Jul 2011; revised 27 Aug 2011; accepted 27 Aug 2011; published 12 Sep 2011

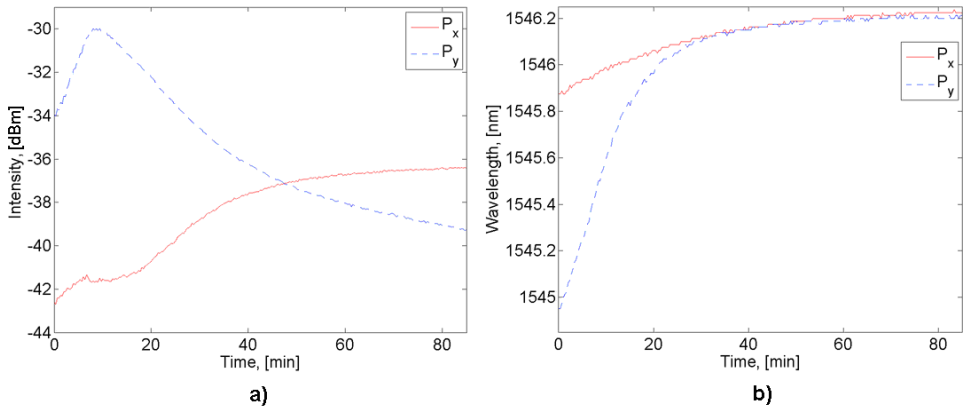

Fig. 4. Evolution of a pair of orthogonally polarized resonances at 1545 nm: amplitude (a) and wavelength (b).

The thickness measurements were done with an AFM microscope (Fig. 5(a)). Several samples were extracted from the plating solution after been exposed to the deposition solution at different plating times to monitor the growth of the film. The thickness of the film was measured by mechanically scratching the film surface and measuring the film's height variation at the boundary as shown in Fig. 5(b) (the red arrow shows the step height at the film boundary).

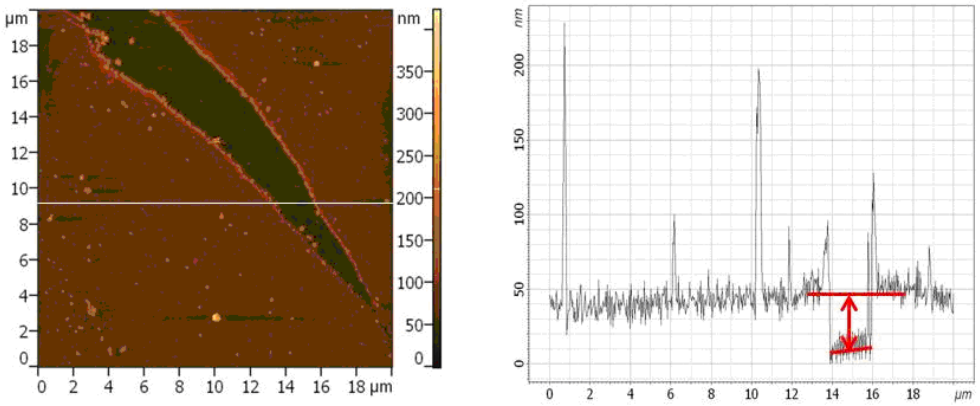

Fig. 5. AFM image (taken after 27 min of deposition) (left), and trace scan (right) showing the thickness variation on the boundary of the scratched area.

The thickness of the film as a function of plating time is shown in Fig. 6(a). It is noted that initial growth of the nanoparticles is initially fast giving the film a thickness of 12 nm in 1 min. The film growth slowed down in the course of plating and eventually reached a plateau after 40 min of deposition, for a final thickness of 60 nm. The observed growth plateau is due to a decrease in the inherent surface free energy of the 10 nm gold nanoparticle seeds. The surface free energy of the particles decreases as the dimensions of particles increase [29].

The correlation between the film thickness and the optical sensor response is shown in Fig. 6(b). The P_y polarization state was chosen, as it has the biggest dynamic range and monotonic growth in comparison to other polarization states. The change in the optical response is almost linear up to about 50 nm of thickness with a correlation factor of 1nm of wavelength shift per 20 nm of film thickness change. The correlation decreases as the thickness exceeds 50 nm, when the film becomes too thick and the optical field cannot tunnel

#151467 - $15.00 USD Received 20 Jul 2011; revised 27 Aug 2011; accepted 27 Aug 2011; published 12 Sep 2011

efficiently all the way to the outer surface. Note the relatively large errors on measurements as the films are quite rough and their thickness difficult to determine with high precision.

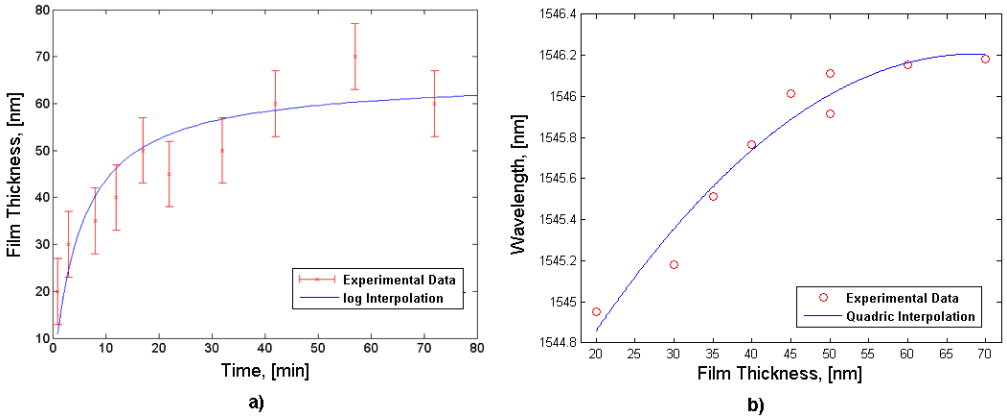

Fig. 6. (a) Time evolution of the average gold film thickness extracted from AFM measurements on individual samples. (b) Correlation between the film thickness and the optical response of the sensor acquired at the P_y polarization state at 1545 nm wavelength.

Before moving on to the thickness optimization results, the film morphology was studied with scanning electron microscopy (Fig. 7).

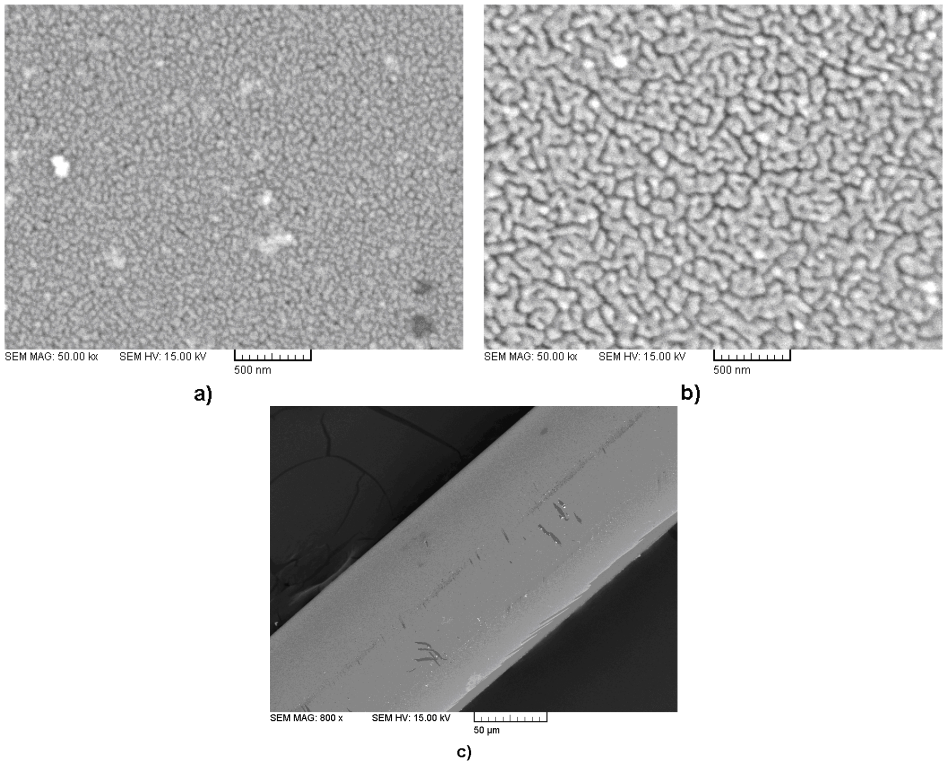

Fig. 7. SEM images of electroless gold plating of the fiber's surface. (1) after 1 min of deposition (2) after 45 min of deposition, (c) image of the fiber's circumference after 40 min of deposition.

The shape of the initial gold particles is spheroid but during electroless plating the metal coating assumes a complex structure with an agglomeration of randomly interconnected plates

#151467 - $15.00 USD Received 20 Jul 2011; revised 27 Aug 2011; accepted 27 Aug 2011; published 12 Sep 2011

that have relatively large (100s of nm) lateral dimensions relative to the overall film thickness (about 40 nm for Fig. 7(b)). The RMS surface roughness of the final films is 5.17 nm

In spite of this small scale granularity (and some physical scratches that were made after deposition on this sample) a larger scale image (Fig. 7(c)) shows that the deposited film coats the fiber surface uniformly. The question now arises whether these films can support surface plasmons that have sufficient quality to be used in sensing applications.

3.2 Thickness optimization

Although the techniques presented above can be calibrated to monitor the film growth, it is quite obvious that they are not precise enough to obtain the optimal film thickness for SPR excitation. To overcome this problem a second technique based on a different analysis of the full TFBG spectrum envelope has been developed.

As shown in an earlier publication [21], the information from the two orthogonal polarizations P_x and P_y can be combined in a single spectrum by introducing the Polarization Dependent Loss (PDL) parameter defined as:

$$PDL(\lambda) = \left| 10Log_{10}\left(\frac{T_x(\lambda)}{T_y(\lambda)}\right)\right| \quad (1)$$

where T_x, and T_y are the transmission spectra for the P_x and P_y polarization states. It was demonstrated that when the metal coating has a thickness for which a plasmon wave can be excited by cladding modes, the PDL spectrum acquires a deep "notch" that reveals the SPR location, and that can be monitored in sensing applications. We now use this characteristic feature of the PDL spectrum to identify the precise moment of the plating process at which the SPR signature is optimized. When the spectral notch is maximized, the thickness is optimal for SPR operation.

This is best observed in the density plot of Fig. 8, where the envelopes of the PDL spectra are represented as a colour scale in the horizontal direction and different plating times (vertical direction). These spectra were obtained in a different experiment from the one reported in the preceding section (although the results of that section could have been processed in the same manner). The chemical concentrations used as well as the size of the plating bath were somewhat larger in the second experiment, resulting in faster plating rates. Indeed, it can be clearly seen that after only approximately 7 min of gold film deposition a deep notch in the PDL envelope occurs (darkest blue colour in Fig. 8(a)). The individual PDL spectrum corresponding to this plating time is shown as Fig. 8(b), while Fig. 8(c) extracts the time evolution of the PDL value at the wavelength where the SPR is observed. The optimum point is clearly seen in the latter figure and provides a tool to interrupt the plating process as soon as a local PDL envelope minimum is reached, regardless of the plating rate. A movie showing the time evolution of the actual PDL spectra is also provided to illustrate more clearly how strongly and suddenly the SPR signature appears during the plating. Figure 8(c) further shows that the PDL envelope evolution slows down gradually for longer plating times (similar to the behavior of the individual loss resonances observed in the first experiment). These effects are due to both the self-termination of the plating process and to the fact that as the metal layer becomes thicker it eventually shields the light from the cladding modes from the outside medium so that further thickness growth is not detected.

#151467 - $15.00 USD Received 20 Jul 2011; revised 27 Aug 2011; accepted 27 Aug 2011; published 12 Sep 2011

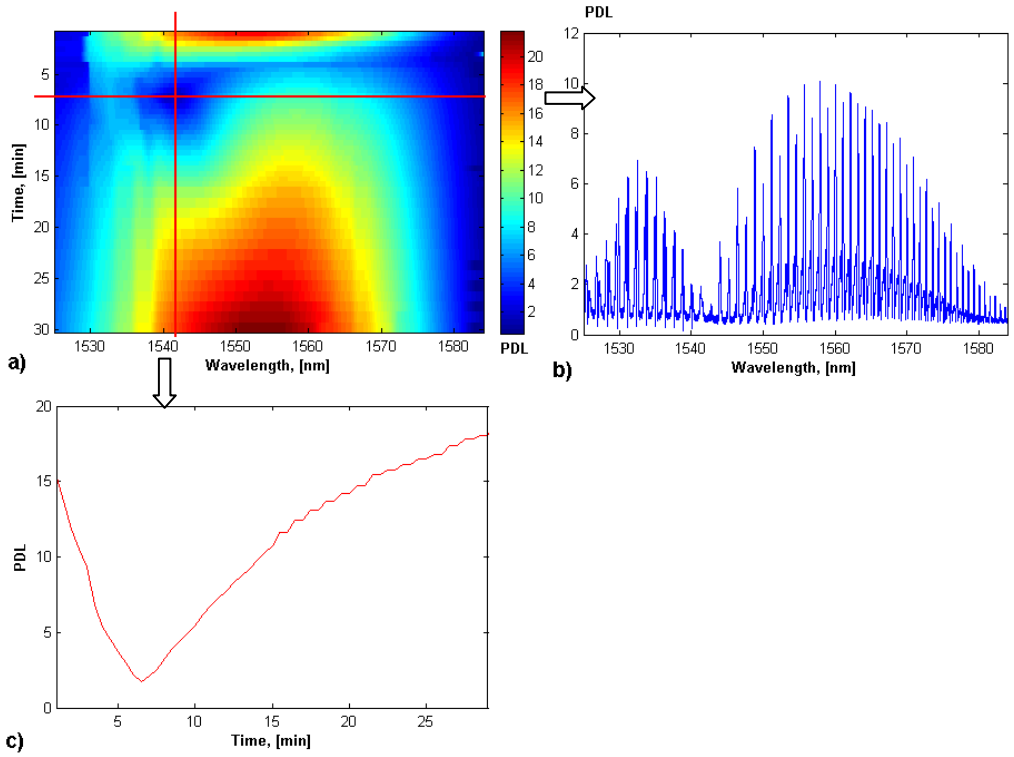

Fig. 8. (a) The envelope of PDL spectra, taken continuously along the course of gold film deposition, and cross sections centered at the point of the deepest notch: wavelength = 1542 nm (b) and time = 7 min (c). (Media 1) The time-lapse evolution of Fig. 8(b) during plating.

4. Conclusion

Electroless plating of gold on optical fibers using nanoparticle seeds attached to the fiber followed by reduction of gold from chloroauric acid in solution has been demonstrated. Plating is a batch process in which large numbers of devices can be coated simultaneously. Plating is also a conformal process, whereas all exposed surfaces of the same material in the plating bath are coated simultaneously and uniformly. Therefore, plating is an ideal method to coat optical fibers with nanoscale layers of metals. Here, gold films with sufficient thicknesses (40 to 60 nm) and uniformity for the realization of fiber SPR sensors have been obtained. Using Tilted Fiber Bragg gratings, we have presented two methods to monitor the growth of the plated film in situ and in real time. The time evolution of the resonance wavelengths of certain cladding modes has been shown to follow the growth of the film thickness. Most importantly however, we showed that by monitoring a simple parameter in the Polarization Dependent Loss of the TFBG during plating, the optimum film thickness for SPR operation can be found with great accuracy, regardless of the plating rate. Obviously this method only applies to the optimum conditions for SPR in water solutions (i.e. similar to the plating bath), and at the wavelengths where the interrogation is carried out. However these conditions are fairly typical for fiber SPR sensor applications in general. It must be pointed out that although we used the TFBG-SPR platform [21] to perform these experiments the monitoring and optimization process can be applied to other types of fiber SPR devices (such as those in [11]) since plating is a batch process in which the TFBG could be inserted amongst other kinds of sensors being plated simultaneously. It is also likely that other metals could be plated and monitored in similar fashion. The method is inherently limited in thickness since the evanescent field of the cladding modes must tunnel across to the outer surface of the metal

#151467 - $15.00 USD Received 20 Jul 2011; revised 27 Aug 2011; accepted 27 Aug 2011; published 12 Sep 2011

film in order to detect changes in thickness. When the thickness exceeds the penetration depth of the light, the thickness growth appears to saturate. Obviously for the application of fiber SPR, the thickness needed must be smaller than the penetration depth, so this does not present an actual limitation in this case. For each type of metal coating, it is possible to predict the optimum SPR thickness and the resulting SPR wavelength with very good accuracy by using planar models (such as the one described in [30]) because the outside surface of the fiber has a radius of curvature that is large relative to the wavelength.

One last observation is that the plated films are relatively rough on the scale of their thickness (RMS roughness close to 10% of the thickness), but that a high quality SPR signature was obtained nevertheless.

Acknowledgments

Financial support from NSERC, the Canada Research Chairs program, and the Institut National d'Optique (Québec) is gratefully acknowledged. C. Caucheteur is supported by the Belgian F.R.S.-FNRS.

#151467 - $15.00 USD Received 20 Jul 2011; revised 27 Aug 2011; accepted 27 Aug 2011; published 12 Sep 2011